WATER RESOURCES RESEARCH, VOL. 32, NO. 9, PAGES 2683–2696, SEPTEMBER 1996

Estimating unsaturated soil hydraulic properties from tension disc infiltrometer data by numerical inversion

J. Šimůnek and M. T. van Genuchten

U.S. Salinity Laboratory, U.S. Department of Agriculture, Agricultural Research Service, Riverside, California

Abstract. Tension disc infiltrometers are becoming increasingly popular devices for in situ measurement of the unsaturated hydraulic properties of soil. Tension infiltration data are generally used to evaluate the parameters K_s and α in Gardner's exponential model of the unsaturated hydraulic conductivity. Either two measurements using different disc diameters or measurements with a single disc but using multiple pressure heads are then used. In this paper we describe a parameter estimation procedure which combines the Levenberg-Marquardt nonlinear parameter optimization method involving weighted least squares, with a quasi-three-dimensional numerical model which solves the variably saturated flow equation. By numerical inversion of Richards' equation the unknown parameters in van Genuchten's model of the unsaturated soil-hydraulic properties are estimated from observed cumulative infiltration data during transient water flow. Additional measurements of the pressure head or water content, as well as a penalty function for constraining the unknown parameters to remain in some feasible region (Bayesian estimation), can be optionally included into the parameter estimation procedure. The problem of optimal sampling design, that is, selecting the best points in space and time for making measurements, is addressed by studying the sensitivity of the objective function to changes in the optimized hydraulic parameters. We calculate objective functions based on available cumulative infiltration, pressure head, and water content measurements and also on several combinations of these data. The behavior of the objective function in three-dimensional parameter space is evaluated by means of a series of two-dimensional response surfaces. The utility of the parameter estimation procedure is demonstrated using numerically generated data. The sensitivity of the procedure to different initial estimates of the model parameters is also discussed.

Introduction

Reliable application of computer models to field-scale flow and transport problems demands a commensurate effort in quantifying a large number of model parameters. As increasingly more complicated flow and transport models are being developed, the accuracy of numerical simulation depends upon the accuracy with which various model parameters are estimated. Knowledge of the unsaturated soil hydraulic properties is especially important when numerical models are used to simulate variably saturated water flow and contaminant transport. Such simulations are generally based on the numerical solutions of Richards' equation, which requires information about the soil water retention, $\theta(h)$, and unsaturated hydraulic conductivity, $K(h)$, functions involving the water content θ, the hydraulic conductivity K, and the soil-water pressure head h. Accurate measurement of these hydraulic properties is confounded by the extreme spatial heterogeneity of the subsurface environment. The hydraulic properties frequently also show significant variations in time because of cultivation or other agricultural activities, shrink-swell phenomena of fine-textured soil, the effect of particle dispersion and soil crusting, and changes in the concentration and ionic composition of the soil solution [*van Genuchten and Šimůnek*, 1996].

A variety of laboratory and field methods are available for direct measurement of the hydraulic conductivity, K, or the soil water diffusivity, D, as a function of the pressure head and/or the water content [*Klute and Dirksen*, 1986; *Green et al.*, 1986]. Most laboratory methods are steady state procedures based on direct inversion of Darcy's law. Transient methods generally involve some type of approximation or simplification of the Richards' equation. Popular transient methods include the *Bruce and Klute* [1956] horizontal infiltration method and various modifications thereof, such as the hot air method and the sorptivity method. Popular field methods include the instantaneous profile method, various unit-gradient-type approaches, sorptivity methods following ponded infiltration, and the crust method based on steady water flow. While relatively simple in concept, these direct measurement methods have a number of limitations that restrict their use in practice. For example, most methods are very time consuming because of the need to adhere to relatively strict initial and boundary conditions. This is especially true for field gravity-drainage experiments involving medium- and fine-textured soils or layered profiles. Methods requiring repeated steady state flow situations or other equilibrium conditions are also tedious, while linearizations and other approximations or interpolations to allow analytic or semianalytic inversions of the flow equation introduce additional errors. Finally, information about uncertainty in the estimated hydraulic parameters is not readily obtained using direct inversion methods.

A more flexible approach for solving the inverse problem is the use of parameter optimization methods. Optimization pro-

Paper number 96WR01525.

cedures also make it possible to simultaneously estimate the retention and hydraulic conductivity functions from transient flow data [*Kool et al*., 1987]. Early parameter optimization studies focused primarily on solute transport [e.g., *van Genuchten*, 1981; *Parker and van Genuchten*, 1984]. Having started with the studies of *Zachmann et al*. [1981] and *Dane and Hruska* [1983], the method is now increasingly being used also for estimating the unsaturated soil hydraulic functions. Computer models applicable to laboratory column outflow measurements have been given by *Kool et al*. [1985a, b] and *Parker et al*. [1985] for one-step outflow procedures and by *van Dam et al*. [1992, 1994] and *Eching and Hopmans* [1993] for multistep approaches. Considerable attention has also been given to the estimation of soil-hydraulic properties from ponded infiltration experiments [*Russo et al*., 1991; *Bohne et al*., 1992]. While initially applied to laboratory-type experiments, inverse methods are equally well applicable to field data [*Kool and Parker*, 1988] or some appropriate combination of field and laboratory data. An important advantage of inverse procedures, if formulated within the context of a parameter optimization problem, is that a detailed error analysis of the estimated parameter is more easily considered. While parameter optimization methods provide several advantages, a number of problems related to computational efficiency, convergence, and parameter uniqueness remain to be solved, especially when many hydraulic parameters must be estimated simultaneously [*van Genuchten and Leij*, 1992].

Tension disc infiltrometers are increasingly being used for in situ measurement of the unsaturated soil hydraulic properties [e.g., *Perroux and White*, 1988; *Ankeny et al*., 1991; *Reynolds and Elrick*, 1991; *Logsdon and Jaynes*, 1993]. Tension infiltrometers are especially useful for quantifying the effects of macropores and preferential flow paths on infiltration in the field. Thus far, tension infiltration data have been used primarily for evaluating the saturated hydraulic conductivity K_s and the sorptivity parameter α in Gardner's exponential model [*Gardner*, 1958] of the unsaturated hydraulic conductivity,

$$K(h) = K_s \exp(\alpha h) \tag{1}$$

Analyses of this type require either two infiltration measurements using two different disc diameters [*Smettem and Clothier*, 1989] or measurements using a single disc diameter but then imposing multiple tensions [*Ankeny et al*., 1991]. The parameters K_s and α are generally estimated using *Wooding*'s [1968] equation for unconfined steady state infiltration from a disc,

$$Q(h_0) = \pi r_0^2 K(h_0) + 4 r_0 \phi(h_0) \tag{2}$$

where Q is the steady state infiltration rate, r_0 is the radius of the disc, h_0 is the wetting pressure head, and ϕ is the matrix flux potential or, equivalently, the linearized Kirchhoff transform given by [*Gardner*, 1958]

$$\phi(h_0, h_i) = \int_{h_i}^{h_0} K(h)\, dh \tag{3}$$

in which h_i is the initial pressure head. Equation (2) considers the two main forces driving the infiltration process: the first term represents one-dimensional gravity-driven flow, while the second term accounts for capillary-induced flow [*Wooding*, 1968]. Explicit in (2) is the assumption that the hydraulic conductivity at the initial pressure head is much lower than the hydraulic conductivity at the wetting pressure head and therefore can be neglected. Since (2) contains two unknown parameters, K and ϕ, or K_s and α after using (1) and (3), the equation has to be written twice for two different experiments as explained above, using two different disc diameters or two different tensions, unless one of the parameter can be estimated independently. For this purpose *White and Sully* [1987] defined the matrix flux potential in terms of the sorptivity which they estimated from early-time infiltration data. However, extreme care is needed in certain cases to properly define the time interval during which the relation between the cumulative infiltration and the square root of time is linear, with sorptivity being the proportionality constant [*Quadri et al*., 1994]. In a different approach, *Logsdon and Jaynes* [1993] proposed a regression method by which the parameters K_s and α were fitted simultaneously to more than two measurements involving different wetting pressure heads at the same location.

As compared to the approximate analytical approaches above, relatively little work has been done in simulating unsaturated flow underneath a disc permeameter using more complete numerical solutions of Richards' equation and even less so in attempts to estimate the unsaturated soil hydraulic properties (including the soil-water retention curve) from tension disc infiltration experiments by means of inverse solutions of Richards' equation. *Quadri et al*. [1994] developed a finite difference numerical model for two-dimensional, axisymmetric water flow and solute transport underneath a disc permeameter. They compared numerical results with laboratory data obtained with a 1/4-sector disc permeameter. Good predictions were obtained for the observed water content and Br^- profiles in the sand box as well as for the measured infiltration rate from the disc [*Quadri et al*., 1994]. In an earlier study, *Warrick* [1992] developed a finite element program, "Disc," which he used for comparing steady state and transient axisymetric flow rates underneath a disc permeameter with alternative solutions of Richards' equation.

In this paper we describe a parameter estimation procedure which combines Levenberg-Marquardt nonlinear parameter optimization involving weighted least squares with a quasi-three-dimensional numerical model which solves the variably saturated flow equation. The unknown parameters in van Genuchten's model for the unsaturated soil properties are estimated from observed cumulative infiltration data during transient water flow by numerical inversion of Richards' equation. Additional data, such as measured pressure heads or water contents, as well as a penalty function for constraining the optimized parameters to remain in some feasible region using Bayesian estimation, can be optionally included in the parameter estimation procedure. Objective functions are formulated in terms of cumulative infiltration, pressure head, and water content data, and on a combination of these measurements. The behavior of the objective functions in three-dimensional parameter space is studied by means of a series of response surfaces in two-dimensional parameter planes. The parameter estimation procedure is demonstrated using numerically generated data; the sensitivity of the method to different initial estimates of the model parameters will be discussed also.

One important issue addressed in this paper is the question of whether infiltration data usually collected during tension disc permeameter experiments are sufficient for the parameter estimation procedure or whether additional data are needed to guarantee a unique inverse solution. We will also examine

which additional data should be collected so as to improve the parameter inversion process.

Theory

The governing flow equation for radially symmetric isothermal Darcian flow in a variably saturated isotropic rigid porous medium, under the assumption that the air phase plays an insignificant role in the liquid flow process, is given by the following modified form of Richards' equation [*Warrick*, 1992]:

$$\frac{\partial \theta}{\partial t} = \frac{1}{r}\frac{\partial}{\partial r}\left(rK\frac{\partial h}{\partial r}\right) + \frac{\partial}{\partial z}\left(K\frac{\partial h}{\partial z}\right) + \frac{\partial K}{\partial z} \qquad (4)$$

where r is a radial coordinate, z is vertical coordinate positive upward, and t is time. Equation (4) was solved numerically for the following initial and boundary equations applicable to a disc tension infiltrometer experiment [*Warrick*, 1992]:

$$h(r, z, t) = h_i \qquad t = 0 \qquad (5)$$

$$h(r, z, t) = h_0 \qquad 0 < r < r_0,\ z = 0 \qquad (6)$$

$$-\frac{\partial h(r, z, t)}{\partial z} - 1 = 0 \qquad r > r_0,\ z = 0 \qquad (7)$$

$$h(r, z, t) = h_i \qquad r^2 + z^2 \to \infty \qquad (8)$$

Equation (4), subject to the above initial and boundary conditions, was solved using a quasi-three-dimensional (axisymmetric) finite element scheme as documented by *Šimůnek et al.* [1996]. The numerical solution was based on the mass-conservative iterative scheme proposed by *Celia et al.* [1990].

A model of the unsaturated soil hydraulic properties must be selected prior to application of the numerical solution of Richards' equation. In this study we will limit ourselves to unsaturated soil hydraulic functions of the form [*van Genuchten*, 1980]

$$\theta_e(h) = \frac{\theta(h) - \theta_r}{\theta_s - \theta_r} = \frac{1}{(1 + |\alpha h|^n)^m} \qquad h < 0$$
$$\theta(h) = \theta_s \qquad h \geq 0 \qquad (9)$$

$$K(\theta) = K_s\theta_e^{1/2}[1 - (1 - \theta_e^{1/m})^m]^2 \qquad h < 0$$
$$K(\theta) = K_s \qquad h \geq 0 \qquad (10)$$

where θ_e is the effective water content; θ_r and θ_s denote the residual and saturated water contents, respectively; and α, n, and m $(=1 - 1/n)$ are empirical parameters. Note that α here is different from that used in (1). The hydraulic characteristics defined by (9) and (10) contain five unknown parameters: θ_r, θ_s, α, n, and K_s. The saturated hydraulic conductivity, K_s, is perceived here and in the remainder of the paper as a fitted hydraulic conductivity at zero pressure head. In reality, the saturated hydraulic conductivity might be different from this value owing to the effects of macropores which saturate only after a zero or positive pressure head is applied [*Logsdon et al.*, 1993]. Following *Logsdon and Jaynes* [1993], we view large macropores as not being predictive of hydraulic properties of the bulk soil matrix.

In the analysis below we will assume that the residual and saturated water contents have been measured independently. The values of the shape parameters α and n will be sought by numerical inversion of the flow problem. The saturated hydraulic conductivity K_s (in the sense of being the hydraulic conductivity at or extrapolated to zero pressure head) will be either assumed known through independent measurement or kept as an unknown parameter to be estimated also by numerical inversion of Richards' equation. Since the tension infiltration experiments by definition do not reach the saturated water content, θ_s, and the saturated hydraulic conductivity, K_s, these two parameters are to be interpreted within this study as extrapolated, empirical parameters outside the range of the disc experiment. Also, tension disc infiltration in general is a wetting process (assuming that one can neglect internal drainage at the initial pressure head); the hydraulic parameters in (9) and (10) should represent wetting branches of the unsaturated hydraulic properties.

Formulation of the Inverse Problem

Several direct and indirect methods [*Neuman*, 1973] may be used to carry out the inverse problem of parameter identification. Direct methods formally treat the model parameters as dependent variables in an inverse boundary value problem [*Yeh*, 1986]. By contrast, indirect methods are based upon the minimization of a suitable objective function which expresses the discrepancy between the observed values and the predicted system response. Initial estimates of the parameters are then iteratively improved upon during this minimization process until a desired precision is obtained. The technique used in this paper constitutes such an indirect approach.

When measurement errors follow a multivariate normal distribution with zero mean and covariance matrix $\mathbf{V}$, the likelihood function can be written as [*Bard*, 1974]

$$L(\boldsymbol{\beta}) = (2\pi)^{-n/2}\det{}^{-1/2}\mathbf{V} \cdot \exp\{(-1/2)[\mathbf{q}^* - \mathbf{q}(\boldsymbol{\beta})]^T\mathbf{V}^{-1}[\mathbf{q}^* - \mathbf{q}(\boldsymbol{\beta})]\} \qquad (11)$$

where $L(\boldsymbol{\beta})$ is the likelihood function, $\boldsymbol{\beta} = \{\beta_1, \beta_2, \cdots, \beta_m\}$ is the vector of optimized parameters (e.g., θ_r, θ_s, α, n, and K_s), m is the number of optimized parameters, $\mathbf{q}^* = \{q_1^*, q_2^*, \cdots, q_n^*\}$ is a vector of observations (such as pressure heads h, water contents θ, and/or cumulative infiltration rates Q), $\mathbf{q}(\boldsymbol{\beta}) = \{q_1, q_2, \cdots, q_n\}$ is a corresponding vector of model predictions as a function of the unknown parameters being optimized, and n is the number of observations. The likelihood function $L(\boldsymbol{\beta})$ is defined as the joint probability density function (pdf) of the observations and is considered a function of the unknown parameters $\boldsymbol{\beta}$ [*Bard*, 1974]. The maximum likelihood estimate is that value of the unknown parameter vector $\boldsymbol{\beta}$ which maximizes the value of the same likelihood function. Since the logarithm is a monotonically increasing function of its argument, the value of $\boldsymbol{\beta}$ which maximizes the likelihood function $L(\boldsymbol{\beta})$ also maximizes $\ln L(\boldsymbol{\beta})$ [*Bard*, 1974]. This property of the logarithm is frequently used in parameter identification studies since $\ln L$ is often a simpler function or easier to use than L itself. Equation (1) is hence reformulated as

$$\ln L(\boldsymbol{\beta}) = -\frac{n}{2}\ln(2\pi) - \tfrac{1}{2}\ln(\det\mathbf{V}) - \tfrac{1}{2}[\mathbf{q}^* - \mathbf{q}(\boldsymbol{\beta})]^T\mathbf{V}^{-1}[\mathbf{q}^* - \mathbf{q}(\boldsymbol{\beta})] \qquad (12)$$

The maximum of the likelihood function must satisfy the set of $\boldsymbol{\beta}$ likelihood equations

$$\frac{\partial \ln L(\boldsymbol{\beta})}{\partial \boldsymbol{\beta}} = 0 \qquad (13)$$

If all elements of the covariance matrix $\mathbf{V}$ are known, then the value of the unknown parameter vector $\boldsymbol{\beta}$ which maximizes (12) must minimize the following equation:

$$\Phi(\boldsymbol{\beta}) = [\mathbf{q}^* - \mathbf{q}(\boldsymbol{\beta})]^T\mathbf{V}^{-1}[\mathbf{q}^* - \mathbf{q}(\boldsymbol{\beta})] \quad (14)$$

If something about the distribution of the fitted parameters is known before the inversion, that information can be included into the parameter identification procedure by multiplying the likelihood function by the prior pdf, $p_0(\boldsymbol{\beta})$, which summarizes the prior information. Estimates which make use of prior information are known as Bayesian estimates and lead to the maximizing of a posterior pdf, $p^*(\boldsymbol{\beta})$, given by

$$p^*(\boldsymbol{\beta}) = cL(\boldsymbol{\beta})p_0(\boldsymbol{\beta}) \quad (15)$$

in which c is a constant. The posterior density function is proportional to the likelihood function when the prior distribution is uniform. Inclusion of the prior information leads to the maximization of the following equation for Φ:

$$\Phi(\boldsymbol{\beta}) = [\mathbf{q}^* - \mathbf{q}(\boldsymbol{\beta})]^T\mathbf{V}^{-1}[\mathbf{q}^* - \mathbf{q}(\boldsymbol{\beta})] + (\boldsymbol{\beta}^* - \hat{\boldsymbol{\beta}})^T\mathbf{V}_\beta^{-1}(\boldsymbol{\beta}^* - \hat{\boldsymbol{\beta}}) \quad (16)$$

where $\boldsymbol{\beta}^*$ is the parameter vector containing the prior information (e.g., θ_r, θ_s, α, n, and K_s), $\hat{\boldsymbol{\beta}}$ is the associated predicted parameter vector, and $\mathbf{V}_\beta$ is a covariance matrix for the parameter vector $\boldsymbol{\beta}$. The second term of (16), sometimes called the penalty function, insures that the obtained estimate is constrained to some feasible region around $\boldsymbol{\beta}^*$ so as to remain physically meaningful. *Russo et al*. [1991] showed that the use of a penalty function can significantly improve the uniqueness of the estimate.

The covariance matrices $\mathbf{V}$ and $\mathbf{V}_\beta$, sometimes also called the weighting matrices, provide information about the measurement accuracy as well as about any possible correlation between measurement errors and between parameters [*Kool et al*., 1987]. When the covariance matrix $\mathbf{V}$ is diagonal and all elements of $\mathbf{V}_\beta$ are equal to zero, that is, the measurement errors are uncorrelated and no prior information about the optimized parameters exists, the problem simplifies to the weighted least squares problem

$$\Phi(\boldsymbol{\beta}) = \sum_{i=1}^{n} w_i[q_i^* - q_i(\boldsymbol{\beta})]^2 \quad (17)$$

where w_i is the weight of a particular measured point.

Solution of the Inverse Problem

Many techniques have been developed in the past to solve the nonlinear minimization/maximization problem [*Bard*, 1974; *Beck and Arnold*, 1977; *Yeh*, 1986; *Kool et al*., 1987]. Most of these methods are iterative by first starting with an initial estimate $\boldsymbol{\beta}_i$ of the unknown parameters to be estimated and then studying how the objective function $\Phi(\boldsymbol{\beta})$ behaves in the vicinity of the initial estimate. On the basis of this behavior, one selects a direction vector $\mathbf{v}_i$ such that the new values of the unknown parameter vector,

$$\boldsymbol{\beta}_{i+1} = \boldsymbol{\beta}_i + \rho_i\mathbf{v}_i = \boldsymbol{\beta}_i - \rho_i\mathbf{R}_i\mathbf{p}_i \quad (18)$$

decreases the value of the objective function

$$\Phi_{i+1} < \Phi_i \quad (19)$$

where Φ_{i+1} and Φ_i are the objective functions at the previous and current iteration level, $\mathbf{R}_i$ is a positive definite matrix, and ρ_i is a scalar that insures that the iteration step is acceptable. Methods based on (18) are called gradient methods. Differences among the various gradient methods presented in the literature (e.g., steepest descent, Newton's method, directional discrimination, Marquardt's method, the Gauss method, variable metric methods, and the interpolation-extrapolation method) are a result of differences in choosing the step direction $\mathbf{v}_i$ and/or the step size ρ_i [*Bard*, 1974]. Steepest descent method selects $\rho_i = 1$ and $\mathbf{R}_i = \mathbf{I}$, where $\mathbf{I}$ is an identity matrix, whereas Newton's method uses $\rho_i = 1$ and $\mathbf{R}_i = \mathbf{H}_i^{-1}$, where $\mathbf{H}$ is the Hessian matrix of $\Phi(\boldsymbol{\beta})$:

$$\mathbf{H}_{ij}(\boldsymbol{\beta}) = \frac{\partial^2\Phi}{\partial\beta_i\partial\beta_j} \quad (20)$$

The Gauss-Newton method simply neglects the higher-order derivatives in the definition of the Hessian matrix and assumes that $\mathbf{H}$ can be approximated by a matrix $\mathbf{N}$ using only the first-order derivatives. For nonlinear weighted least squares this leads to

$$\mathbf{H} \approx \mathbf{N} = \mathbf{J}^T\mathbf{J} \quad (21)$$

in which $\mathbf{J}$ is the Jacobian matrix whose elements are given by the sensitivity coefficients multiplied by a square root of the weight of a particular data point as follows:

$$J_{ij} = \frac{\partial[q_i^* - q_i(\boldsymbol{\beta})]w_i^{1/2}}{\partial\beta_j} = -w_i^{1/2}\frac{\partial q_i(\boldsymbol{\beta})}{\partial\beta_j} \quad (22)$$

Marquardt [1963] proposed a very effective method which has become a standard in nonlinear least squares fitting. The method represents a compromise between the inverse Hessian and steepest descend methods by using the steepest descent method when the objective function is far from its minimum and switching to the inverse Hessian method as the minimum is approached. This switch is accomplished by multiplying the diagonal in the Hessian matrix (or its approximation $\mathbf{N}$), sometimes called the curvature matrix, with $(1 + \lambda)$, where λ is a positive scalar. When λ is large, then the matrix is diagonally dominant resulting in the steepest descend method. On the other hand, when λ is zero, the inverse Hessian method will result.

The sensitivity coefficients may be calculated using three different methods [*Yeh*, 1986]: the influence coefficient method (finite differences), a sensitivity equation method, and a variational method. When using the influence method, one has to balance truncation errors which increase with $\Delta\boldsymbol{\beta}$ against rounding errors in differencing which decrease with $\Delta\boldsymbol{\beta}$. A common practice is to change the optimized parameters by one percent to obtain estimates of the sensitivity coefficients,

$$\frac{\partial q_i}{\partial\beta_j} = \frac{q_i(\boldsymbol{\beta} + \Delta\boldsymbol{\beta}e_j) - q_i(\boldsymbol{\beta})}{\Delta\beta_j} \quad (23)$$

where e_j is the jth unit vector, and $\Delta\boldsymbol{\beta} = 0.01\ \boldsymbol{\beta}$.

Data Generation

Infiltration data describing flow from a tension disc were numerically generated for three hypothetical soils (sand, loam, and clay [*Hillel and van Bavel*, 1976]) and used to evaluate the feasibility of the proposed method for estimating unsaturated

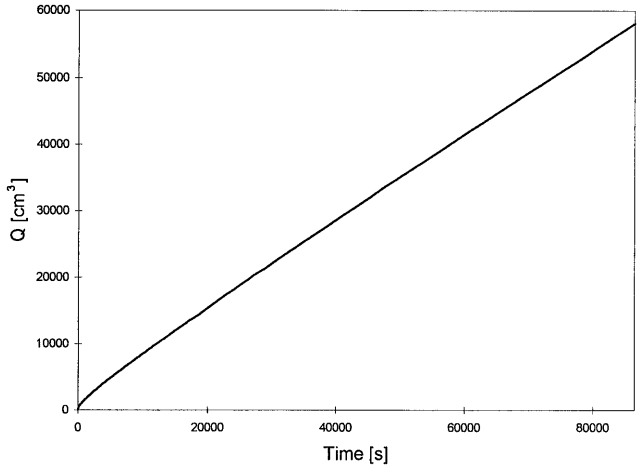

Figure 1. Cumulative infiltration versus time for a hypothetical disc permeameter infiltration experiment.

soil hydraulic parameters. Only results for the loam will be reported here since the results and conclusions obtained for this soil were qualitatively very much the same as those for the hypothetical sand and clay soils.

The soil hydraulic parameters of the hypothetical loam were taken as follows: $\theta_r = 0.000$, $\theta_s = 0.480$, $\alpha = 0.0150$ cm^{-1}, $n = 1.592$, and $K_s = 0.0007$ cm s^{-1}. The radius of the disc permeameter was assumed to be 10 cm. The initial pressure head of the homogeneous and isotropic soil beneath the disc was taken as -500 cm, whereas the pressure head in the disc was set at -3 cm. Only measurements during the first 12 hours of the experiment were included in the analysis below. The ratio of the infiltration rate at 12 hours to those at 24 and 48 hours was 1.021 and 1.039, respectively. This result should signal a caution to field workers since steady state infiltration was apparently not reached during the first 12 hours. Still, the relatively small changes in infiltration rate in this example after 12 hours are probably negligible from a practical point of view.

We will follow an analysis somewhat different than that used previously by *Kool and Parker* [1988], who considered a hypothetical one-dimensional ponded infiltration experiment followed by redistribution and evapotranspiration. Our analysis involves the following steps and calculations.

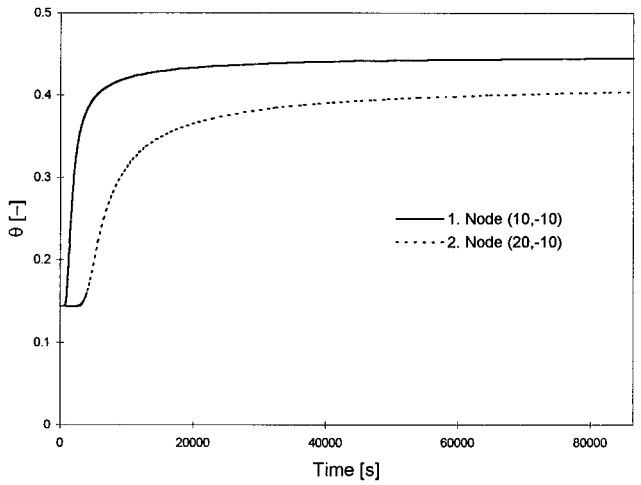

Figure 2. Calculated water content versus time at two observation nodes, $(r, z) = (10, -10)$ and $(20, -10)$, for the hypothetical disc permeameter infiltration experiment.

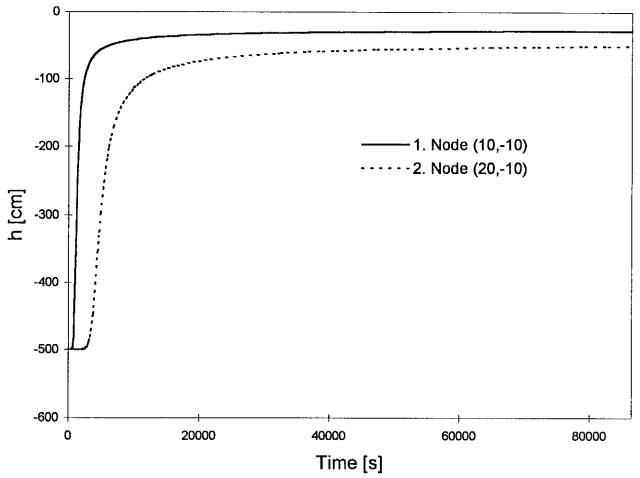

Figure 3. Calculated pressure head versus time at two observation nodes, $(r, z) = (10, -10)$ and $(20, -10)$, for the hypothetical disc permeameter infiltration experiment.

1. The known hypothetical soil-hydraulic properties $\theta(h)$ and $K(h)$ were first used in the direct problem to simulate the tension disc infiltration event for given initial and boundary conditions. The finite element discretization was selected so that the mass balance error for the direct solutions always remained less than 0.05%.

2. The instantaneous and cumulative (Figure 1) infiltration rates that were generated were discretized at given times, whereas the calculated water content (Figure 2) and pressure head (Figure 3) profiles were sampled at two given locations, again at discrete times. Both nodes were at 10 cm depth, one at the edge of the disc, the other at twice the radius. In this study we used local nodal values of the pressure head and water content for the hypothetical observations. We emphasize, however, that experimental devices for measuring h and θ, such as tensiometers and time domain reflectometry, have always some finite length rather than yielding point measurements, that is, they average the measured variable over a finite volume of soil:

$$\bar{\theta}(r, z, t) = \frac{1}{V}\int_V \theta(r, z, t)\, dV$$
$$\bar{h}(r, z, t) = \frac{1}{V}\int_V h(r, z, t)\, dV \tag{24}$$

where $\bar{\theta}$ and $\bar{h}$ are the spatial averages of the water content and pressure head, respectively, over a volume V representing the averaging volume of the particular measurement device. Integrating pressure heads or water contents over a given volume around a specified location for a particular measurement device should not pose any significant numerical problem as such. However, interesting questions could be raised, such as in what direction the measurement devices should be placed (horizontally or vertically) to obtain the greatest benefit in terms of parameter identification [*Vogeler et al.*, 1996], or whether the simultaneous measurement of both horizontally and vertically averaged pressure heads or water contents could provide ad-

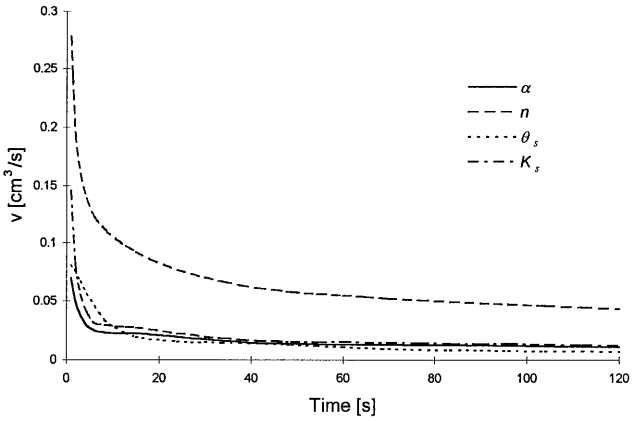

Figure 4. Sensitivity of the instantaneous infiltration rate, $v(t)$, to a 1% change in hydraulic parameters α, n, θ_s, and K_s.

ditional information for improving parameter identifiability (B. E. Clothier, personal communication, 1996). Since these questions go beyond the scope of this paper, they will not be further addressed here. Infiltration rates were calculated as the sum of the actual nodal fluxes Q_i associated with nodes having prescribed Dirichlet boundary conditions representing the disc permeameter. The nodal fluxes could be calculated explicitly and accurately from the original finite element equations associated with these nodes [*Šimůnek et al.*, 1996]. The cumulative disc permeameter infiltration rate, $Q(t)$, was calculated as follows:

$$Q(t) = \int_{t_0}^{t} v(t)\, dt = \int_{t_0}^{t} \sum_{i=1}^{n} Q_i(t)\, dt \tag{25}$$

where t_0 is the starting time of the experiment, $v(t)$ is the instantaneous infiltration rate, and n is the number of nodes representing the disc permeameter.

3. The data obtained in steps 1 and 2 were used to calculate sensitivities of the objective function to the optimized parameters. A similar study on behavior of sensitivities in the one-dimensional advection-dispersion equation was carried out by *Knopman and Voss* [1987].

4. The data obtained in steps 1 and 2 were next used to calculate response surfaces of the objective function as a function of a particular hydraulic parameter or a combination of parameters so as to determine possible uniqueness problems of the inverse procedure.

5. The data obtained in steps 1 and 2 were used as input data for the inverse problem. In a first group of inversions, instantaneous infiltration rates, cumulative infiltration data, or additional "data" (water contents and pressure heads measured at a given location) were used individually, without any additional information. Combinations of these primary measurement sets were subsequently used in a second group of inversions to evaluate whether additional information would substantially improve the error estimates on the parameters as well as on the goodness of fit. Sensitivities to the initial parameter estimates were also studied. Sensitivity coefficients in this study were calculated using the Levenberg-Marquardt method, combined with the influence coefficient method.

Experimental Design

In general, experiments should be designed such that measurements are made which yield the most information about the unknown parameters to be optimized, that is, measurements which are most sensitive to changes in the unknown parameters. The sensitivity of the objective function to the optimized parameters is usually studied in terms of sensitivity coefficients as given by (23). Unfortunately, sensitivity coefficients calculated in this manner are difficult to compare with each other since they depend on the absolute values of the hydraulic parameters involved as well as on the invoked units. Therefore we will evaluate the sensitivities in a different way so as to remove their dependency on parameter units and absolute values:

$$e_{ij} = 100\beta_j \left| \frac{\partial q_i}{\partial \beta_j} \right| = 100\beta_j \frac{|q_i(\boldsymbol{\beta} + \Delta\boldsymbol{\beta} e_j) - q_i(\boldsymbol{\beta})|}{1.01\beta_j - \beta_j}$$

$$= |q_i(\boldsymbol{\beta} + \Delta\boldsymbol{\beta} e_j) - q_i(\boldsymbol{\beta})| \tag{26}$$

where e_{ij} is the change in the auxiliary variable q_i corresponding to a 1% change in parameter β_j.

Figure 4 shows the sensitivity of the instantaneous infiltration rate, $v(t)$, to 1% changes in the parameters α, n, θ_s, and K_s. Since the residual water content was assumed to be zero, we did not use θ_r in our sensitivity study. Because of physical considerations, we expected that there would be a certain time interval $(0, t_{\text{grav}})$ at the beginning of the infiltration event during which the infiltration rate would be very sensitive to the unknown parameters. The characteristic time t_{grav} would define the point in time when gravity starts dominating the infiltration process [*Warrick*, 1992]. Figure 4 shows that the infiltration rate is very sensitive to changes in all four parameters at only very short times, that is, less than 10 s. After that, the sensitivity of the infiltration rate becomes essentially constant and almost independent of time. Since it is practically impossible to obtain several measurements within such a short time period immediately after initiating the infiltration event, v is not a recommended variable for use in the inverse problem and hence will not be further considered here for calculating response surfaces.

The sensitivities of the cumulative infiltration, $Q(t)$, to 1% changes in the hydraulic parameters is presented in Figure 5. Notice that the sensitivities increase with time for all four

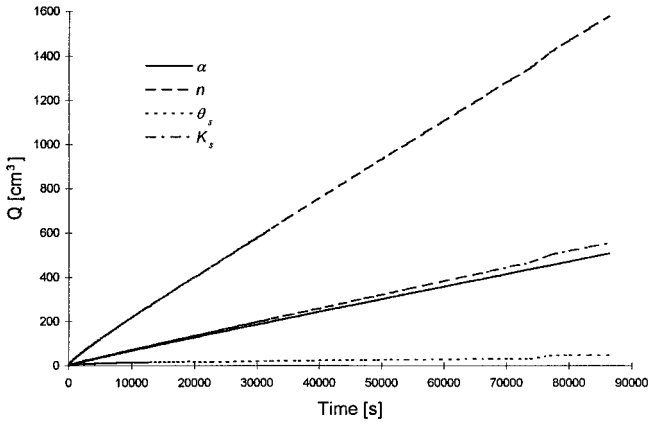

Figure 5. Sensitivity of the cumulative infiltration rate, $Q(t)$, to a 1% change in hydraulic parameters α, n, θ_s, and K_s.

parameters. The cumulative infiltration rate is most sensitive to the parameter n and least to the saturated water content θ_s. The sensitivity to n is about three times higher than the sensitivities to α and the saturated hydraulic conductivity K_s, which are about the same. If the absolute values in (26) were to be removed, the sensitivity to α would get a sign opposite to that of K_s. When comparing the sensitivities to the different parameters, it is important to recognize that a 1% change in parameter n, which can change in order of units and therefore 1% change covers larger range of possible values, will be much more important than a 1% change in K_s, which can vary several orders of magnitude in the field. The results presented in Figure 5 suggest that the further in time the measurements are taken the more valuable the information becomes, with the limiting situation occurring when steady state has been reached.

Figure 6 presents the sensitivity of the pressure head, h, to the hydraulic parameters α, n, θ_s, and K_s at observation nodes (r, z) located at (10, −10) (Figure 6a) and (20, −10) (Figure 6b), that is, one node slightly slanted below the disc and one right below the edge of the permeameter. The highest sensitivities of the pressure head at both observation nodes occur during the time period when the moisture front passes through these points. As with the cumulative infiltration rate, 1% changes in n induce the biggest changes in the pressure head, although the sensitivities to the other three parameters are not much smaller. The sensitivities of h are about the same at the two observation nodes, although the second node located further to the side of the source maintains its high sensitivity for a much longer time period because of a more diffuse moisture front. Hence, as compared to measurement points below the source, locations at the side of the disc should yield more information for the inverse problem, but this will be at the expense of a prolonged experimental effort and more computer time. In practice, a compromise between these two locations may be needed. Still, whatever the location of measurement, data of the pressure head should be taken when the moisture front passes through that location.

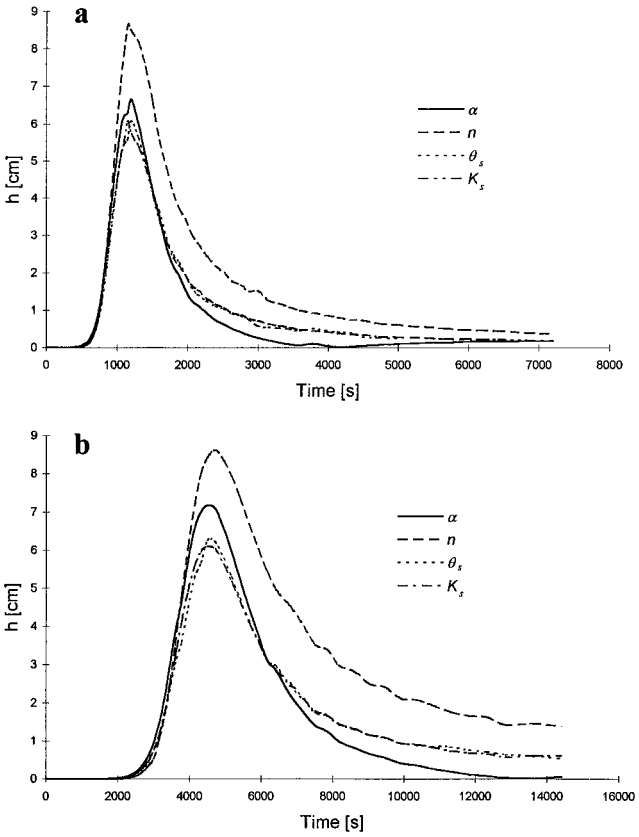

Figure 6. Sensitivity of the pressure head at two observation nodes (a) $(r, z) = (10, -10)$ and (b) $(r, z) = (20, -10)$ to a 1% change in hydraulic parameters α, n, θ_s, and K_s.

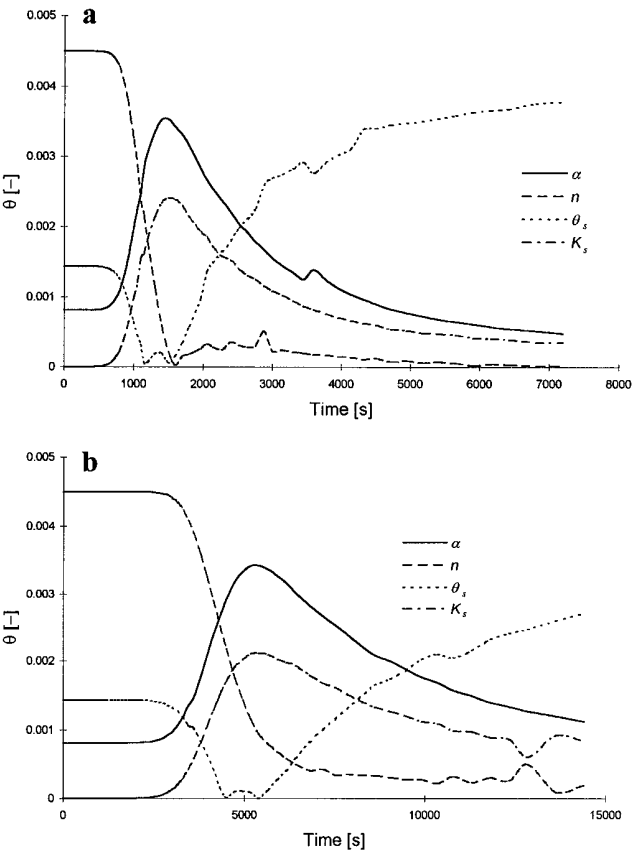

Figure 7. Sensitivity of the water content at two observation nodes (a) $(r, z) = (10, -10)$ and (b) $(r, z) = (20, -10)$ to a 1% change in hydraulic parameters α, n, θ_s, and K_s.

Sensitivities of the water content to α, n, θ_s, and K_s at the same two observation nodes, $(r, z) = (10, -10)$ and (20, −10), are shown in Figure 7. The initial sensitivities of θ before arrival of the moisture front are caused by the initial condition being prescribed in terms of the pressure head. This condition causes the water content at early times to be sensitive to all parameters used in the description of the retention curve (α, n, θ_s) but not to the saturated hydraulic conductivity, K_s. The water content during passage of the moisture front is very sensitive to α and K_s but not very sensitive to n and θ_s. After passage of the moisture front the sensitivity to α and K_s decreases gradually, although more slowly than for the pressure head (Figure 6). By contrast, the sensitivity to the saturated water content θ_s increases after passage of the moisture front; this is to be expected since the soil water content is now slowly approaching (and hence defining) the value of θ_s. Since the water content remains sensitive to at least one hydraulic parameter during the entire infiltration event, water content mea-

Table 1. Grid Spacings Used for the Parameter Planes of the Hypothetical Disc Permeameter Infiltration Experiment

Parameter	Lower Parameter Value	Parameter Step Value	Upper Parameter Value
α, cm^{-1}	0.002	0.002	0.06
n [−]	1.0333	0.03333	2.0
K_s, cm s^{-1}	0.00001	0.00005	0.0015

surements should cover the entirety of the infiltration experiment.

The results presented in Figures 4 through 7 can be interpreted in two different ways. First, observed data should be taken at points in time and space which show the highest sensitivities of those observations to the hydraulic parameters and which are easily accessible to measure. The inverse procedure will not improve by including in the objective function data which are insensitive to the parameters to be optimized. For example, including pressure head data measured before the arrival or after passage of the moisture front will not improve the identifiability of the hydraulic parameters since they will lead to similar predicted pressure heads during those times. Second, higher weights should be placed on "measurements" with show the highest sensitivity to the optimized parameters, and relative small weights should be placed on other, more insensitive observations.

Response Surfaces

Russo et al. [1991] reported for a one-dimensional ponded infiltration experiment that the cumulative infiltration curve does not provide enough information to obtain a unique set of optimized parameters. Similar results were also obtained for one-step outflow experiments when only the outflow curve was used in the inverse problem [*van Dam et al*., 1992, 1994; *Eching and Hopmans*, 1993; *Toorman et al*., 1992] except when relative large pressures were imposed on the samples so as to provide a high resolution in the average water content of the sample [*Parker et al*., 1985]. Additional information of the pressure head inside of the sample provided enough information to successfully apply the inverse problem by yielding a unique set of optimized parameters. In this section we test whether the conventionally measured data on cumulative infiltration rate from a disc permeameter provide enough information to enable the identification of a unique set of soil hydraulic parameters from the inverse problem and, if not, what additional information is necessary to successfully carry out the inversion. We will approach this question in a way similar to that of *Toorman et al*. [1992] in their study of the uniqueness of the inverse problem for one-dimensional one-step outflow experiments.

The uniqueness of the inverse problem will be evaluated in terms of two-dimensional response surfaces of the objective function as a function of pairs of soil-hydraulic parameters. The objective function used for this purpose is given as

$$\Phi(\boldsymbol{\beta}, \mathbf{q}_m) = \sum_{j=1}^{m} \left(w_j \sum_{i=1}^{n_j} w_i [q_j^*(t_i) - q_j(t_i, \boldsymbol{\beta})]^2 \right) \quad (27)$$

where m represents the different sets of measurements, that is, those involving cumulative infiltration, pressure head, or water content data; n_j is the number of measurements in a particular set; $q_j^*(t_i)$ are specific measurements at time t_i for the jth measurement set; $q_j(t_i, \boldsymbol{\beta})$ are the corresponding model predictions for the parameter vector $\boldsymbol{\beta}$; and w_j and w_i are weights associated with a particular measurement set or point, respectively. We assumed that the weighting coefficients w_i in (27) are equal to 1, that is, the variances of the errors inside of a particular measurement set are the same. The weighting coefficient for the water content set as a whole, w_θ, was also set equal to 1, while those for the cumulative infiltration, w_Q, and the pressure head, w_h, sets were defined as

$$w_h = \left[\frac{\sum_{j=1}^{n_\theta} q_{\theta j}^*}{n_\theta} \right] \left[\frac{\sum_{i=1}^{n_h} q_{hi}^*}{n_h} \right]^{-1} \quad (28)$$

$$w_Q = \left[\frac{\sum_{j=1}^{n_\theta} q_{\theta j}^*}{n_\theta} \right] \left[\frac{\sum_{i=1}^{n_Q} q_{Qi}^*}{n_Q} \right]^{-1} \quad (29)$$

respectively, where n_θ, n_h, and n_Q represent the total number of measurements obtained for the water content, pressure head, and cumulative infiltration, respectively; and q_θ^*, q_h^*, and q_Q^* are the actual measurements of θ, h, and Q, respectively.

We calculated the objective functions for three parameter planes (i.e., α-n, α-K_s, and n-K_s), for three separate sets of measurements (i.e., for cumulative infiltration, pressure head, and water content data), and for four combined sets of data (i.e., $Q + h + \theta$, $Q + h$, $Q + \theta$, and $h + \theta$). The response surfaces were calculated on a rectangular grid with parameter values given in Table 1. Each parameter domain was discretized into 30 discrete points, resulting in 900 grid points for each response surface. A total of more than 60 response surfaces was calculated in this manner (three soil types, although only the loam results are presented here, and three two-dimensional parameter planes for each of three types of separate or four combined data measurements).

Figure 8 represents response surfaces of the objective function $\Phi(Q)$ for the cumulative infiltration measurements (see also Figure 1) for the three different parameter planes, α-n, α-K_s, and n-K_s. The α-n response surface (Figure 8a) shows a well-defined valley which starts at low α and n values and extends linearly through nearly the entire parameter space. Notice that we decreased the distance between the contour levels toward the low values of the objective function so as to more precisely locate the minimum of $\Phi(Q)$. We obtained visually almost identical response surface in the parameter plane α-K_s (Fig. 8b), although now several local minima appeared for relatively small values of the parameters α and K_s. Figures 8a and 8b indicate that a higher value of α and corresponding increases in n or K_s will lead to very similar values of the objective function, thus indicating possible difficulties in finding a unique inverse solution. Figure 8c also displays a well-defined narrow valley, now of hyperbolic shape, suggesting an inverse relationship between the parameters n and K_s in terms of their effect on the objective function. An increase in n and a corresponding decrease in K_s will produce the same response in the objective function. This hyperbolic behavior of $\Phi(Q)$ indicates that the saturated hydraulic conductivity is more identifiable when n is relatively large (e.g., greater than about 1.4), while n is similarly better identifiable when K_s is

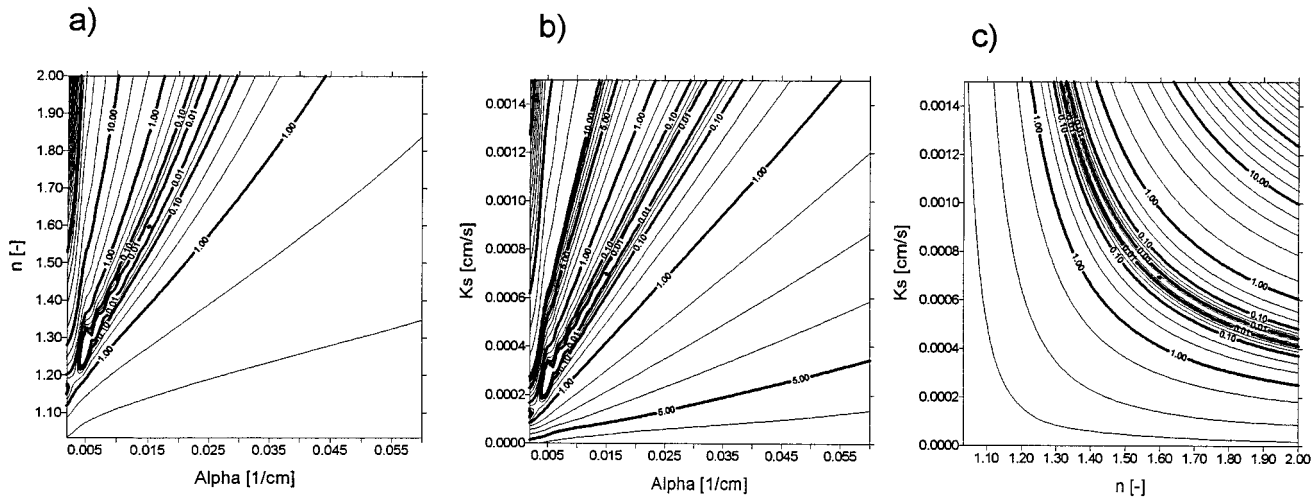

Figure 8. Contours of the objective function $\Phi(Q)$ for the cumulative infiltration rate in the (a) α-n plane, (b) α-K_s plane, and (c) n-K_s parameter plane.

large (e.g., >0.008 cm/s). When n is larger than about 1.4, a small change in the saturated hydraulic conductivity results in a relatively large change in the objective function. The same is true for the parameter n when the saturated hydraulic conductivity is large. The nonexistence of a well-defined minimum in the response surfaces in Figure 8 permits a broadening of the conclusion of *Russo et al.* [1991] that identical infiltration curves for one-dimensional ponded infiltration can be generated by an infinite number of combinations of parameters α, n, and K_s. His conclusion holds also in three dimensional space for tension disc permeameters.

Figure 9 represents response surfaces of $\Phi(h)$ for the pressure head measured at $(r, z) = (20, -10)$ (Figure 3), again in the three parameter planes α-n, α-K_s, and n-K_s. The response surfaces for the h-based objective function, $\Phi(h)$, are visually quite similar to those for the cumulative infiltration rate, $\Phi(Q)$. An increase in α and a simultaneous increases in K_s or n again lead to approximately the same values for the objective function. The contours of $\Phi(h)$ and the valley around its minimum in Figure 9a are almost parallel with the n axis, thus indicating that the parameter n is very difficult to identify from available information. And similarly, as $\Phi(Q)$ in Figure 8c, the pressure head based objective function $\Phi(h)$ reacts inversely to an increase in the parameters n and K_s (Figure 9c). The contours of $\Phi(h)$ at relatively low values of K_s, as well as the long valley around the minimum, are almost parallel with the n axis (Figure 9c), thus showing that n can not be identified precisely when all three parameters α, n, and K_s are to be estimated simultaneously. Still, the minimum of $\Phi(h)$ is somewhat better identifiable than the minimum of $\Phi(Q)$.

Figure 10 shows similar response surfaces for the objective function $\Phi(\theta)$ for the water content measured at $(r, z) = (20, -10)$ (Figure 2). The objective function $\Phi(\theta)$ has very well defined minima in all three parameter planes. Increased identifiability of the parameters is partly caused by the fact that the initial condition was specified in terms of the pressure head. Adding one water content measurement will then cause one point of the retention curve to become known.

The response surfaces shown thus far are for objective functions associated with only one measured variable: Q, h, or θ.

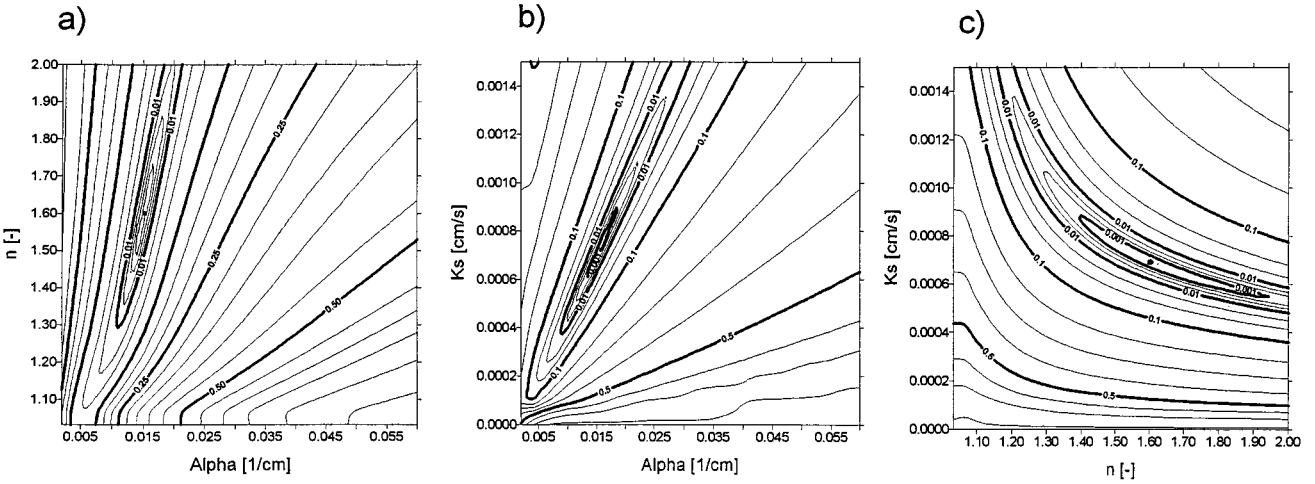

Figure 9. Contours of the objective function $\Phi(h)$ for the pressure head measured at $(r, z) = (20, -10)$ in the (a) α-n plane, (b) α-K_s plane, and (c) n-K_s parameter plane.

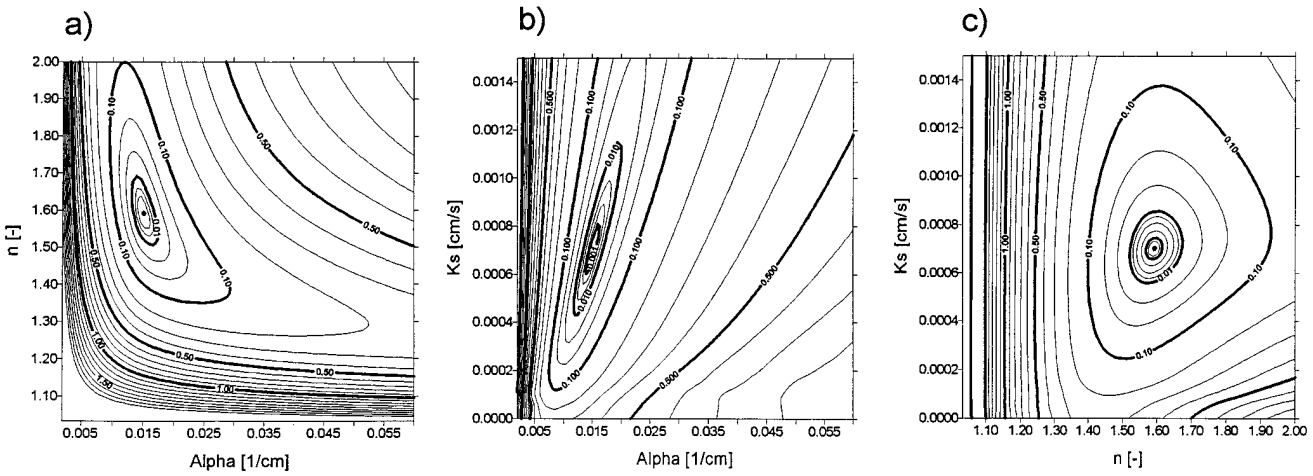

Figure 10. Contours of objective function $\Phi(\theta)$ for the water content measured at $(r, z) = (20, -10)$ in the (a) α-n plane, (b) α-K_s plane, and (c) n-K_s parameter plane.

We now address the question whether the identifiability of the parameters will increase when the objective functions for two variables are combined. Figure 11 presents in all three parameter planes the contours of the objective function $\Phi(Q, h)$ $(=\Phi(Q) + \Phi(h))$ defined by both the cumulative infiltration and the pressure head measured at $(r, z) = (20, -10)$. One can readily see that the identifiability of the parameters does not markedly increase in comparison with the response surfaces of the separate objective functions $\Phi(Q)$ and $\Phi(h)$. This result is mainly due to the similarity of the response surfaces when the two variables are considered separately. Figures 8 and 9 show that the valleys surrounding the minima in both cases have almost an identical shape; hence simply adding the two objective functions will not improve the definition of the minima. A more optimal inverse scenario would be if the valleys of the response surfaces surrounding the minima were perpendicular for the two variables, thereby improving the definition of the minima when the objective functions are combined. This is not the case here where combination of the objective functions for the pressure head and the cumulative infiltration actually resulted in several local minima in the parameter planes α-n and α-K_s (Figures 11a and 11b).

Better results are obtained when the objective functions based on the cumulative infiltration, $\Phi(Q)$, and the water content measured at $(r, z) = (20, -10)$, $\Phi(\theta)$, are combined. Figure 12 shows that the response surfaces for this objective function $\Phi(Q, \theta)$ are now well defined in all three planes (α-n, α-K_s, and n-K_s). An exception is perhaps the α-K_s plane, which shows a valley that extends over a relative wide range of α and K_s values. Finally, and for completeness, we also present in Figures 13 and 14 contours of objective functions $\Phi(h, \theta)$ and $\Phi(Q, h, \theta)$, respectively, in the three parameter planes. The minima of the objective functions in all the planes are again very well identifiable.

Inverse Solutions

To evaluate the robustness of the parameter optimization procedure and the dependence of the final solution on the initial estimates of the unknown hydraulic parameters, we car-

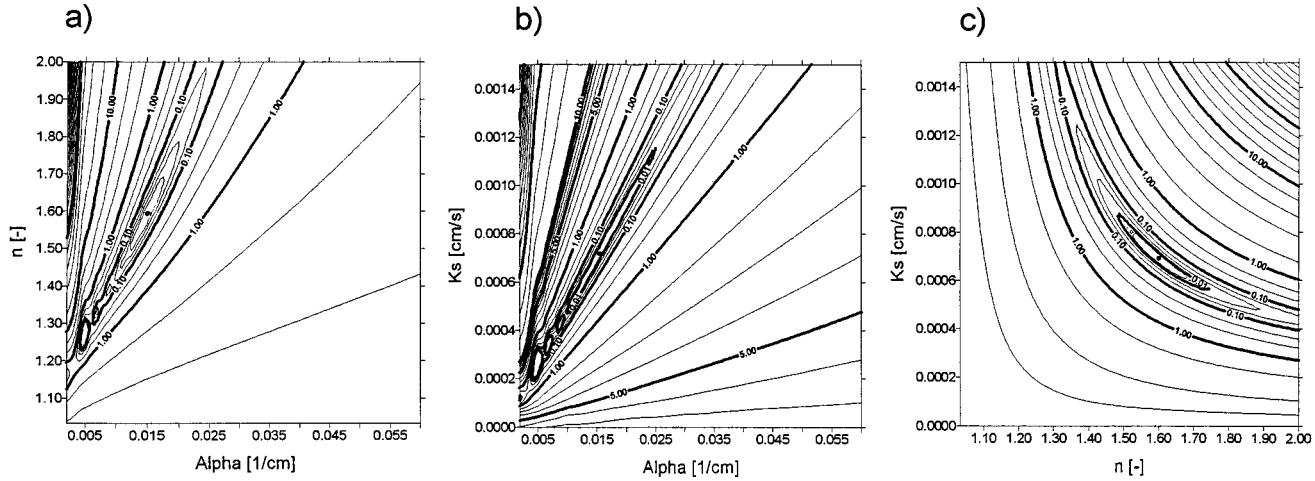

Figure 11. Contours of the objective function $\Phi(Q, h)$ for the cumulative infiltration rate and the pressure head measured at $(r, z) = (20, -10)$ in the (a) α-n plane, (b) α-K_s plane, and (c) n-K_s parameter plane.

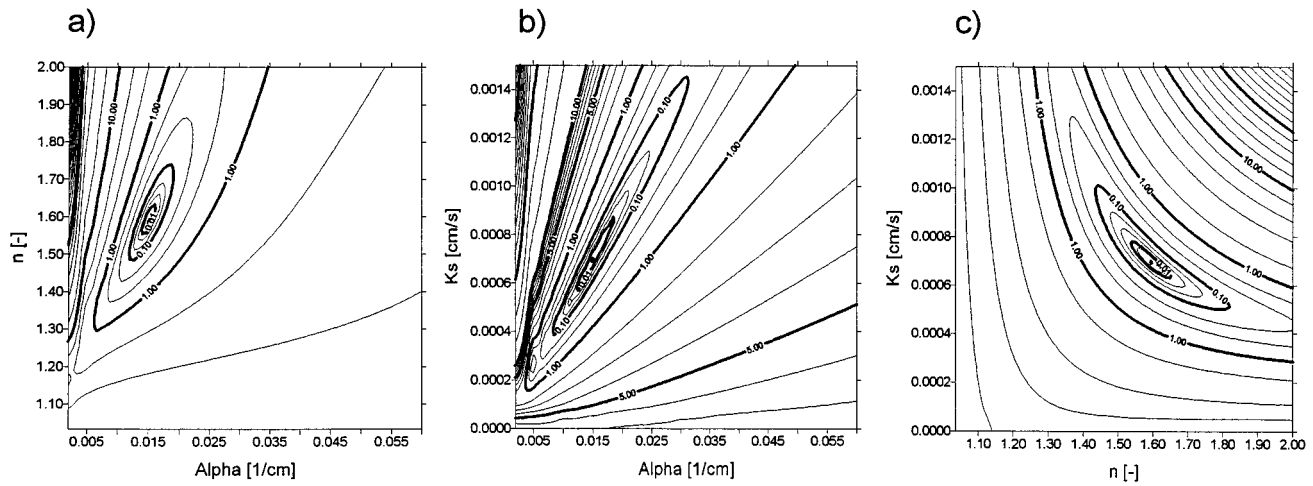

Figure 12. Contours of the objective function $\Phi(Q, \theta)$ for the cumulative infiltration rate and the water content measured at $(r, z) = (20, -10)$ in the (a) α-n plane, (b) α-K_s plane, and (c) n-K_s parameter plane.

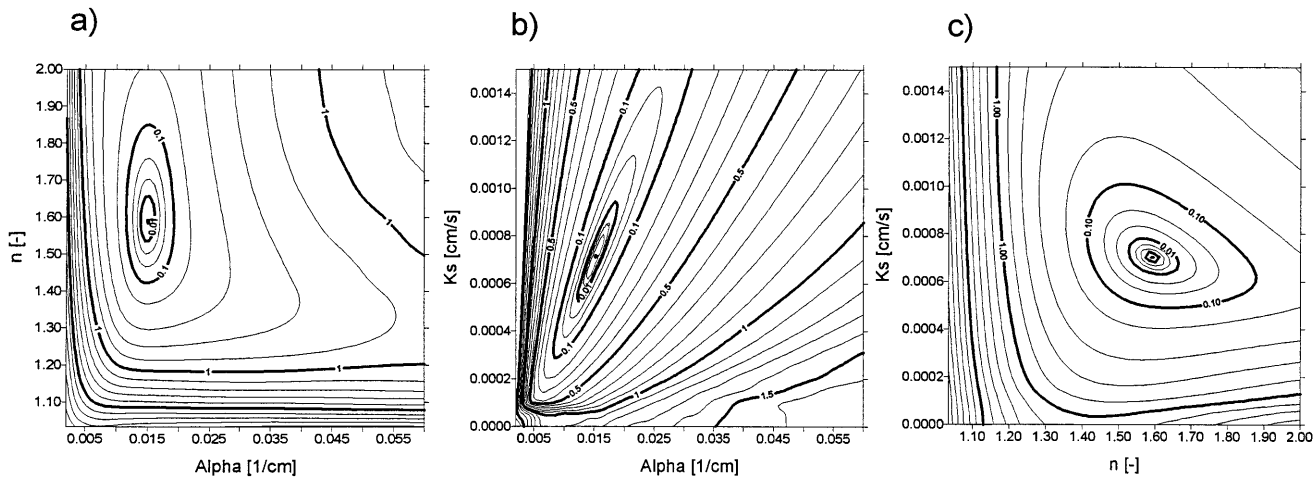

Figure 13. Contours of the objective function $\Phi(h, \theta)$ for the water content and the pressure head measured at $(r, z) = (20, -10)$ in the (a) α-n plane, (b) α-K_s plane, and (c) n-K_s parameter plane.

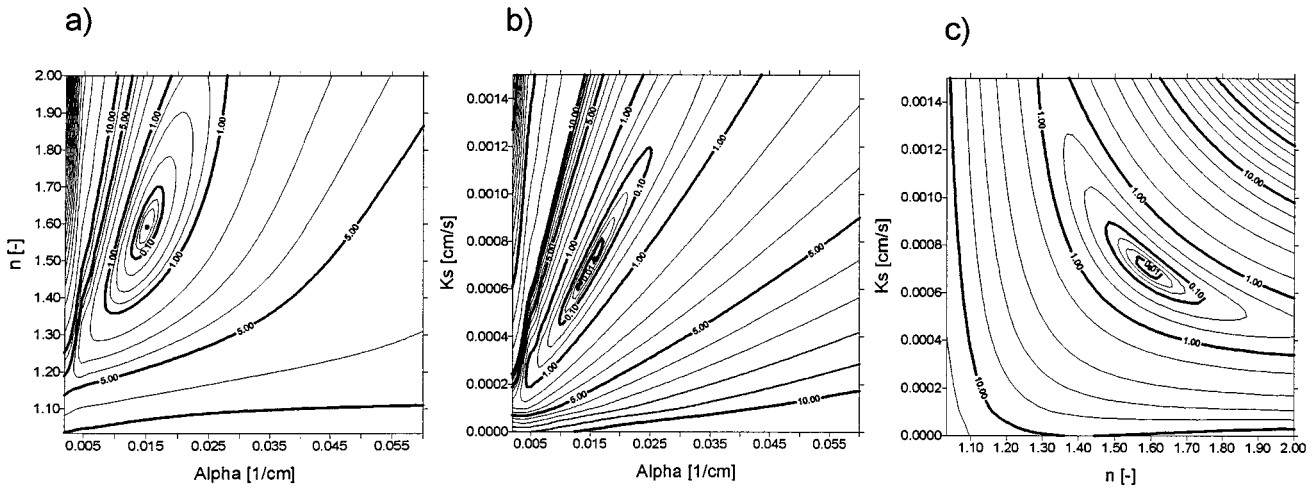

Figure 14. Contours of the objective functions $\Phi(Q, h, \theta)$ for the cumulative infiltration, the water content and the pressure head measured at $(r, z) = (20, -10)$ in the (a) α-n plane, (b) α-K_s plane, and (c) n-K_s parameter plane.

Table 2. Results Obtained With the Different Parameter Estimation Computer Runs

Case	Fitted Parameter	Measurement Sets	Initial Estimates			Final Estimates			Φ
			α	n	K_s	α	n	K_s	
1a*	α, n, K_s	v	0.02	1.25	0.0001	0.00922	1.715	0.00036	0.1718e−02
b*	α, n, K_s	v	0.03	1.66	0.0001	0.00916	1.716	0.00036	0.1719e−02
c*	α, n, K_s	v	0.006	1.12	0.0001	0.00902	1.722	0.00035	0.1853e−02
2a	α, n	v	0.02	1.25	⋯	0.01508	1.594	⋯	0.9209e−04
b	α, n	v	0.03	1.66	⋯	0.01547	1.605	⋯	0.4022e−03
c	α, n	v	0.006	1.12	⋯	0.01507	1.594	⋯	0.9260e−04
3a*	α, n, K_s	Q	0.02	1.25	0.0001	0.01038	1.677	0.00043	0.3482e+05
b*	α, n, K_s	Q	0.03	1.66	0.0001	0.02187	3.195	0.00037	0.3181e+05
c*	α, n, K_s	Q	0.006	1.12	0.0001	0.00935	1.640	0.00041	0.2113e+05
4a	α, n	Q	0.02	1.25	⋯	0.01493	1.589	⋯	0.8023e+04
b*	α, n	Q	0.03	1.66	⋯	0.02398	1.931	⋯	0.2283e+05
c	α, n	Q	0.006	1.12	⋯	0.01501	1.592	⋯	0.5087e+04
5a*	α, n, K_s	h_1	0.02	1.25	0.0001	0.00761	1.010	0.00057	0.5309e+05
b	α, n, K_s	h_1	0.03	1.66	0.0001	0.01510	1.580	0.00071	0.4485e−00
c	α, n, K_s	h_1	0.006	1.12	0.0001	0.01502	1.592	0.00070	0.1326e−02
6a	α, n	h_1	0.02	1.25	⋯	0.01502	1.592	⋯	0.1386e−02
b	α, n	h_1	0.03	1.66	⋯	0.01502	1.592	⋯	0.7290e−03
c	α, n	h_1	0.006	1.12	⋯	0.01502	1.592	⋯	0.9520e−04
7a*	α, n, K_s	θ_1	0.02	1.25	0.0001	0.01057	1.712	0.00042	0.2598e−04
b*	α, n, K_s	θ_1	0.03	1.66	0.0001	0.00991	1.739	0.00038	0.2232e−04
c*	α, n, K_s	θ_1	0.006	1.12	0.0001	0.02003	1.519	0.00107	0.3984e−04
8a	α, n	θ_1	0.02	1.25	⋯	0.01503	1.592	⋯	0.2845e−04
b	α, n	θ_1	0.03	1.66	⋯	0.01503	1.592	⋯	0.2850e−04
c	α, n	θ_1	0.006	1.12	⋯	0.01504	1.592	⋯	0.2891e−04
9a	α, n, K_s	Q, h_1	0.02	1.25	0.0001	0.01507	1.592	0.00070	0.9381e+01
b*	α, n, K_s	Q, h_1	0.03	1.66	0.0001	0.01475	3.500	0.00025	0.5243e+05
c	α, n, K_s	Q, h_1	0.006	1.12	0.0001	0.01497	1.596	0.00070	0.9209e+01
10a	α, n	Q, h_1	0.02	1.25	⋯	0.01502	1.592	⋯	0.8755e+01
b	α, n	Q, h_1	0.03	1.66	⋯	0.01503	1.592	⋯	0.8751e+01
c	α, n	Q, h_1	0.006	1.12	⋯	0.01503	1.593	⋯	0.9996e+01
11a*	α, n, K_s	Q, θ_1	0.02	1.25	0.0001	0.01038	1.719	0.00041	0.1285e−03
b	α, n, K_s	Q, θ_1	0.03	1.66	0.0001	0.01552	1.583	0.00073	0.4281e−04
c*	α, n, K_s	Q, θ_1	0.006	1.12	0.0001	0.01930	1.528	0.00101	0.1100e−03
12a	α, n	Q, θ_1	0.02	1.25	⋯	0.01502	1.592	⋯	0.3714e−04
b	α, n	Q, θ_1	0.03	1.66	⋯	0.01502	1.592	⋯	0.3714e−04
c	α, n	Q, θ_1	0.006	1.12	⋯	0.01502	1.592	⋯	0.3716e−04
13a	α, n, K_s	h_1, θ_1	0.02	1.25	0.0001	0.01503	1.592	0.00070	0.2870e−04
b	α, n, K_s	h_1, θ_1	0.03	1.66	0.0001	0.01503	1.593	0.00070	0.2870e−04
c	α, n, K_s	h_1, θ_1	0.006	1.12	0.0001	0.01504	1.593	0.00070	0.2875e−04
14a	α, n	h_1, θ_1	0.02	1.25	⋯	0.01503	1.592	⋯	0.2870e−04
b	α, n	h_1, θ_1	0.03	1.66	⋯	0.01502	1.592	⋯	0.2870e−04
c	α, n	h_1, θ_1	0.006	1.12	⋯	0.01503	1.592	⋯	0.2871e−04
15a	α, n, K_s	Q, h_1, θ_1	0.02	1.25	0.0001	0.01498	1.593	0.00070	0.3744e−04
b	α, n, K_s	Q, h_1, θ_1	0.03	1.66	0.0001	0.01498	1.593	0.00070	0.3739e−04
c	α, n, K_s	Q, h_1, θ_1	0.006	1.12	0.0001	0.01497	1.593	0.00070	0.3734e−04
16a	α, n	Q, h_1, θ_1	0.02	1.25	⋯	0.01502	1.592	⋯	0.3717e−04
b	α, n	Q, h_1, θ_1	0.03	1.66	⋯	0.01502	1.592	⋯	0.3825e−04
c	α, n	Q, h_1, θ_1	0.006	1.12	⋯	0.01502	1.592	⋯	0.3716e−04
17a	α, n, K_s	Q, h_1, h_2, θ_1, θ_2	0.02	1.25	0.0001	0.01471	1.598	0.00068	0.5297e−04
b	α, n, K_s	Q, h_1, h_2, θ_1, θ_2	0.03	1.66	0.0001	0.01451	1.604	0.00067	0.7173e−04
c	α, n, K_s	Q, h_1, h_2, θ_1, θ_2	0.006	1.12	0.0001	0.01501	1.593	0.00070	0.3682e−04
18a	α, n	Q, h_1, h_2, θ_1, θ_2	0.02	1.25	⋯	0.01502	1.592	⋯	0.3557e−04
b	α, n	Q, h_1, h_2, θ_1, θ_2	0.03	1.66	⋯	0.01502	1.592	⋯	0.3565e−04
c	α, n	Q, h_1, h_2, θ_1, θ_2	0.006	1.12	⋯	0.01502	1.592	⋯	0.3557e−04
Real parameters		⋯	⋯	⋯	⋯	0.01502	1.592	0.00070	⋯

*Unsuccessful runs.

ried out 18 different optimization runs. The various optimization cases differed in terms of the number of parameters being optimized and the information used to define the objective function. Either all three parameters α, n, and K_s (cases 1, 3, ⋯, 17) or only the shape parameters α and n (cases 2, 4, 6, ⋯, 18) were fitted. Similarly, as for the response surfaces, we used for the inverse procedure the objective functions defined by the three different sets of measurements, that is, the cumulative infiltration (cases 3 and 4), the pressure head (cases 5 and 6), the water content (cases 7 and 8), or certain combinations of these measurements ($Q + h$ for cases 9 and 10; $Q + \theta$ for cases 11 and 12; $h + \theta$ for cases 13 and 14; $Q + h + \theta$ for cases 15 and 16 with one observation node; and $Q + h + \theta$ for cases 17 and 18 with two observation nodes). In addition, we used the infiltration rates for the inverse solution (cases 1 and 2). Each optimization case was repeated three times using different initial estimates of the shape parameters α and n.

Results of the different parameter estimation runs are summarized in Table 2. Unsuccessful runs, whose cases are marked by an asterisk, are defined as those where the optimized parameters deviated by more than 5% from the true value. Note that with only one exception, all inversion attempts involving only the two parameters α and n were successful. The exception was a case where only cumulative infiltration data were used to define the objective function. Using different initial estimates for the same case actually did produce the correct hydraulic parameter values.

The results were far less successful when all three parameters α, n, and K_s were optimized simultaneously, yielding unsuccessful runs in 13 out of 27 cases. The low success rate was fully expected when the parameters were estimated from either the instantaneous or cumulative infiltration curve (these two curves should roughly hold the same information). As we discussed earlier, the same infiltration curve can be calculated using an infinite number of combinations of values for α, n, and K_s. However, we were somewhat surprised to have several unsuccessful runs when parameters were optimized using the objective functions $\Phi(\theta)$ or $\Phi(Q, \theta)$ since the response surfaces for these two objective functions (Figures 10 and 12) showed relatively well-defined minima. This result may be explained in two ways. First, the contours of $\Phi(\theta)$ in Figure 10b as well as the valley around the minimum are almost parallel to the K_s axis, thus suggesting that the solution will not be very sensitive to the values of the saturated hydraulic conductivity. Second, the α-n, α-K_s, and n-K_s planes represent only three two-dimensional cross sections of the full three-dimensional parameter space. The behavior of the objective function in these three planes can only suggest how the objective function might behave in the rest of the three-dimensional space. Other local minima of the objective function Φ may exist which do not show up with the three cross-sectional planes. To verify this explanation, we calculated several additional response surfaces for the α-n parameter plane but now assuming different values for K_s (plots not further shown here). Several local minima of the type shown in Figure 8a and also visible in Figures 11a and 11b were found on these additional plots. We note that some of the very small local minima on these and other plots may have been caused also, or exacerbated, by minor oscillations in the numerical results. Still, our study indicates that having well-defined minima in the three two-dimensional parameter planes does not automatically guarantee that no other local minima are present and hence that the hydraulic parameters obtained by the inverse solution are always unique.

Conclusions

We have developed a numerical code for identifying soil-hydraulic parameters from unsaturated flow data typically observed during a three-dimensional disc permeameter infiltration experiment. The results presented in this study indicate that measurements of the instantaneous or cumulative infiltration rates alone will not provide a unique solution in the three-dimensional parameter space α-n-K_s. An analysis of inverse solutions shows that similar conclusion also hold for the water content when measured at only one or two locations in the field. Although the response surfaces for the objective function based on the water content showed well-defined minima in each of the three selected parameter planes (α-n, α-K_s, and n-K_s), additional local minima in three-dimensional parameter space still caused nonuniqueness in the optimized parameters. Additional information of the pressure head measured in the profile significantly increased the uniqueness of the solution. Actually, using only pressure head measurements already guaranteed convergence to the correct parameters. Having a combination of the objective functions for the pressure head and the cumulative infiltration rate did not improve the finale fit. Best identifiability was obtained when both the pressure head and the water content were measured simultaneously. In this case the simultaneously measured pressure head and water content data should directly define several points of the retention curve, in which case the saturated hydraulic conductivity becomes the main unknown parameter driving the inverse solution process.

Identification of the two shape parameters α and n was successful using any combination of measurements. This finding suggests that it may be possible to obtain from disc permeameter experiments the saturated hydraulic conductivity (in the sense of the unsaturated conductivity as extrapolated to zero pressure head) based on the traditional analysis of *Wooding* [1968] and the assumption of having a Gardner-type exponential unsaturated hydraulic conductivity function and to identify only the shape parameters α and n in the retention curve by inverse solution of Richards' equation.

Finally, we emphasize that this study was conducted using numerically generated synthetic data. No additional noise was added to the generated data to reflect measurement or calibration errors, which are unavoidable in experimental studies. Additional studies of how measurement errors will affect the results may need to be carried out before the inverse technique should be used with real data.

Acknowledgment. Thanks are due to one anonymous and one not-so-anonymous (B. E. Clothier) reviewer for their many useful suggestions and comments.

References

Ankeny, M. D., M. Ahmed, T. C. Kaspar, and R. Horton, Simple field method for determining unsaturated hydraulic conductivity, *Soil Sci. Soc. Am. J.*, *55*, 467–470, 1991.

Bard, Y., *Nonlinear Parameter Estimation*, 341 pp., Academic, San Diego, Calif., 1974.

Beck, J. V., and K. J. Arnold, *Parameter Estimation in Engineering and Science*, John Wiley, New York, 1977.

Bohne, K., C. Roth, F. J. Leij, and M. T. van Genuchten, Rapid method for estimating the unsaturated hydraulic conductivity from infiltration measurement, *Soil Sci.*, *155*(4), 237–244, 1992.

Bruce, R. R., and A. Klute, The measurement of soil moisture diffusivity, *Soil Sci. Soc. Am. Proc.*, *20*, 458–462, 1956.

Celia, M. A., E. T. Bouloutas, and R. L. Zarba, A general mass-conservative numerical solution for the unsaturated flow equation, *Water Resour. Res.*, *26*(7), 1483–1496, 1990.

Dane, J. H., and S. Hruska, In-situ determination of soil hydraulic properties during drainage, *Soil Sci. Soc. Am. J.*, *47*, 619–624, 1983.

Eching, S. O., and J. W. Hopmans, Optimization of hydraulic functions from transient outflow and soil water pressure data, *Soil Sci. Soc. Am. J.*, *57*, 1167–1175, 1993.

Gardner, W. R., Some steady-state solutions of the unsaturated moisture flow equation with application to evaporation from a water table, *Soil Sci.*, *85*, 228–232, 1958.

Green, R. E., L. R. Ahuja, and S. K. Chong, Hydraulic conductivity, diffusivity, and sorptivity of unsaturated soils: Field methods, in *Methods of Soil Analysis*, *Agron. Monogr. 9*, part 1, 2nd ed., edited by A. Klute, pp. 771–798, Soil Sci. Soc. Am., Madison, Wis., 1986.

Hillel, D., and C. H. M. van Bavel, Simulation of profile water storage as related to soil hydrologic properties, *Soil Sci. Soc. Am. J.*, *40*, 807–815, 1976.

Klute, A., and C. Dirksen, Hydraulic conductivity and diffusivity: Lab-

oratory methods, in *Methods of Soil Analysis*, *Agron. Monogr. 9*, part 1, 2nd ed., edited by A. Klute, pp. 687–734, Soil Sci. Soc. Am., Madison, Wis., 1986.

Knopman, D. A., and C. I. Voss, Behavior of sensitivities in the one-dimensional advection-dispersion equation: Implication for parameter estimation and sampling design, *Water Resour. Res.*, *23*(2), 253–272, 1987.

Kool, J. B., and J. C. Parker, Analysis of the inverse problem for transient unsaturated flow, *Water Resour. Res.*, *24*(6), 817–830, 1988.

Kool, J. B., J. C. Parker, and M. T. van Genuchten, ONESTEP: A nonlinear parameter estimation program for evaluating soil hydraulic properties from one-step outflow experiments, *Bull. Va. Agric. Exp. Stn. 85-3*, 1985a.

Kool, J. B., J. C. Parker, and M. T. van Genuchten, Determining soil hydraulic properties from one-step outflow experiments by parameter estimation, I, Theory and numerical studies, *Soil Sci. Soc. Am. J.*, *49*, 1348–1354, 1985b.

Kool, J. B., J. C. Parker, and M. T. van Genuchten, Parameter estimation for unsaturated flow and transport models—A review, *J. Hydrol.*, *91*, 255–293, 1987.

Logsdon, S. D., and D. B. Jaynes, Methodology for determining hydraulic conductivity with tension infiltrometers, *Soil Sci. Soc. Am. J.*, *57*, 1426–1431, 1993.

Logsdon, S. D., E. L. McCoy, R. R. Allmaras, and D. R. Linden, Macropore characterization by indirect methods, *Soil Sci.*, *155*, 316–324, 1993.

Marquardt, D. W., An algorithm for least-squares estimation of nonlinear parameters, *SIAM J. Appl. Math.*, *11*, 431–441, 1963.

Neuman, S. P., Calibration of distributed parameter groundwater flow models viewed as a multiple-objective decision process under uncertainty, *Water Resour. Res.*, *9*(4), 1006–1021, 1973.

Parker, J. C., and M. T. van Genuchten, Determining transport parameters from laboratory and field tracer experiments, *Bull. Va. Agric. Exp. Stn. 84-3*, 96 pp., 1984.

Parker, J. C., J. B. Kool, and M. T. van Genuchten, Determining soil hydraulic properties from one-step outflow experiments by parameter estimation, II, Experimental studies, *Soil Sci. Soc. Am. J.*, *49*, 1354–1359, 1985.

Perroux, K. M., and I. White, Design for disc permeameters, *Soil Sci. Soc. Am. J.*, *52*, 1205–1215, 1988.

Reynolds, W. D., and D. E. Elrick, Determination of hydraulic conductivity using a tension infiltrometer, *Soil Sci. Soc. Am. J.*, *55*, 633–639, 1991.

Russo, D., E. Bresler, U. Shani, and J. C. Parker, Analysis of infiltration events in relation to determining soil hydraulic properties by inverse problem methodology, *Water Resour. Res.*, *27*(6), 1361–1373, 1991.

Quadri, M. B., B. E. Clothier, R. Angulo-Jaramillo, M. Vauclin, and S. R. Green, Axisymetric transport of water and solute underneath a disk permeameter: Experiments and numerical model, *Soil Sci. Soc. Am. J.*, *58*, 696–703, 1994.

Šimůnek, J., M. Šejna, and M. T. van Genuchten, The HYDRUS-2D software package for simulating water flow and solute transport in two-dimensional variably saturated media, version 1.0, *IGWMC—TPS-53*, Int. Ground Water Model. Cent., Colo. School of Mines, Golden, Colo., 1996.

Smettem, K. R. J., and B. E. Clothier, Measuring unsaturated sorptivity and hydraulic conductivity using multiple disk permeameters, *J. Soil Sci.*, *40*, 563–568, 1989.

Toorman, A. F., P. J. Wierenga, and R. G. Hills, Parameter estimation of hydraulic properties from one-step outflow data, *Water Resour. Res.*, *28*(11), 3021–3028, 1992.

van Dam, J. C., J. N. M. Stricker, and P. Droogers, Inverse method for determining soil hydraulic functions from one-step outflow experiment, *Soil Sci. Soc. Am. Proc.*, *56*, 1042–1050, 1992.

van Dam, J. C., J. N. M. Stricker, and P. Droogers, Inverse method to determine soil hydraulic functions from multistep outflow experiment, *Soil Sci. Soc. Am. Proc.*, *58*, 647–652, 1994.

van Genuchten, M. T., A closed-form equation for predicting the hydraulic conductivity of unsaturated soils, *Soil Sci. Soc. Am. J.*, *44*, 892–898, 1980.

van Genuchten, M. T., Non-equilibrium transport parameters from miscible displacement experiments, *Res. Rep. 119*, U.S. Salinity Lab., U.S. Dep. of Agric., Agric. Res. Serv., Riverside, Calif., 1981.

van Genuchten, M. T., and F. J. Leij, On estimating the hydraulic properties of unsaturated soils, in *Indirect Methods for Estimating the Hydraulic Properties of Unsaturated Soils*, edited by M. T. van Genuchten, F. J. Leij, and L. J. Lund, pp. 1–14, Univ. of Calif., Riverside, 1992.

van Genuchten, M. T., and J. Šimůnek, Evaluation of pollutant transport in the unsaturated zone, in *Proceedings of Regional Approaches to Water Pollution in the Environment*, *NATO ASI Ser., Ser 2, Environment*, edited by P. E. Rijtema and V. Elias, Kluwer, Norwell, Mass., in press, 1996.

Vogeler, I., B. E. Clothier, S. R. Green, D. R. Scotter, and R. W. Tillman, Characterizing water and solute movement by time domain reflectometry and disk permeametry, *Soil Sci. Soc. Am. J.*, *60*, 5–12, 1996.

Warrick, A. W., Model for disc infiltrometers, *Water Resour. Res.*, *28*(5), 1319–1327, 1992.

White, I., and M. J. Sully, Macroscopic and microscopic capillary length and timescales from field infiltration, *Water Resour. Res.*, *23*, 1514–1522, 1987.

Wooding, R. A., Steady infiltration from large shallow circular pond, *Water Resour. Res.*, *4*, 1259–1273, 1968.

Yeh, W. W.-G., Review of parameter identification procedures in groundwater hydrology: The inverse problem, *Water Resour. Res.*, *22*(2), 95–108, 1986.

Zachmann, D. W., P. C. Duchateau, and A. Klute, Simultaneous approximation of water capacity and soil hydraulic conductivity by parameter identification, *Soil Sci.*, *134*, 157–163, 1981.

J. Šimůnek and M. T. van Genuchten, U.S. Salinity Laboratory, U.S. Department of Agriculture, ARS, 450 W. Big Springs Rd., Riverside, CA 92507-4617. (e-mail: jsimunek@ussc.ars.usda.gov)

(Received February 15, 1996; revised May 13, 1996;
accepted May 17, 1996.)